Advances in Science and Technology Research Journal

Advances in Science and Technology Research Journal, 2026, 20(4), 427–444
https://doi.org/10.12913/22998624/215186
ISSN 2299-8624, License CC-BY 4.0

Received: 2025.11.12
Accepted: 2026.02.16
Published: 2026.03.01

Fuzzy-logic expert system based on simulation and experimental research on a pyrotechnically actuated automatic mechanism

Marek Rośkowicz[1], Michał Jasztal[1], Mateusz Kunikowski[1*], Norbert Grzesik[2], Rafał Bazela[3]

[1] Military University of Technology, ul. gen. Sylwestra Kaliskiego 2, 00-908 Warsaw, Poland
[2] Polish Air Force University, ul. Dywizjonu 30335, 08-521 Dęblin, Poland
[3] Military Institute of Armament Technology, ul. Wyszyńskiego 7, 05-220 Zielonka, Poland
* Corresponding author's e-mail: mateusz.kunikowski@wat.edu.pl

ABSTRACT

The results of simulation and experimental research on a pyrotechnically actuated automatic mechanism were presented. A simulation model was constructed in MSC ADAMS. The driving force was determined based on field trial results, which provided the values of the gas pressure in the gas cylinders during the operation of the actual device. Verification of numerically calculated kinematic parameters was based on high-speed camera recordings of the mechanism motion under field conditions. Numerical studies first examined how variations in the gas piston force affected kinematics, then how different friction coefficients influenced motion. The results confirmed the usefulness of the model and its potential for analyzing destructive effects on kinematic and dynamic parameters. All simulations and experiments were used to develop an expert system that assesses how selected factors affect the correctness of mechanism operation. This work may serve as an important tool supporting personnel in the proper handling of this kind of machines.

Keywords: simulation model, MSC ADAMS software, high-speed camera, TEMA software, automatic mechanism powered by pyrotechnics, fuzzy logic.

INTRODUCTION

The subject of study in the presented work is an automatic mechanism powered by a gas-powder engine. The gas pressure generated during the combustion of powder is utilized both for launching the payload and for preparing the mechanism for subsequent operation. The functioning of the mechanism continues as long as the initiation system of the pyrotechnic cartridge is engaged. Such mechanisms in both civilian and military applications are used wherever extremely rapid operation is required. Pyrotechnically driven mechanisms are utilized in a variety of civilian safety systems. However, automatic weapon mechanisms, where operation occurs automatically utilizing a powder charge to perform useful work and drive the system itself are particularly demanding for designers and operators. The displacements of kinematic elements in such mechanisms occur very rapidly, resulting in significant dynamic forces that cause quick wear of these system components. Operational practice indicates that there is often a need to monitor the current technical condition of these devices, especially when their manufacturer has specified only the overall service life of the entire unit. In such situations, it becomes necessary to identify the reliability characteristics of the device, represented by diagnostic parameters and their threshold values [1]. This article presents the research on the kinematic and dynamic parameters of the motion of elements in an automatic mechanism powered by a gas-powder engine. The proposed

research concept is based on minimizing the number of planned experiments through the use of modern computer-aided modeling, calculations, and simulations tools (CAD/CAE) [2,3]. Such software is increasingly employed for modeling and simulating the operation of the dynamic systems discussed in the study [4,5].

This article continues a series of publications dedicated to the use of computer methods and a research platform for analyzing the kinematics and dynamics of a pyrotechnically actuated automatic mechanism. In earlier publications, the process of developing a numerical model [6] and the experimental-numerical analysis of the functioning of the aforementioned device were presented [7].

In this work, the process of expanding the simulation model of the functional system of the device under investigation was presented, followed by its verification through experimental research. The modernization of the numerical model involved, among other things, defining the driving force of the analyzed mechanism based on field trial results. These trials yielded the values of gas pressure in the gas cylinders during the operation of the actual device. Pressure measurement was conducted using specialized piezoelectric sensors designed for such systems with specific ranges of pressure variations and their durations [8,9]. Additionally, verification of the kinematic parameters of the mechanism motion obtained through computer simulation was conducted by recording the operation of real mechanisms using a high-speed camera (under field conditions) [10,11]. The footage recorded with this device was then analyzed using the specialized TEMA software [12,13]. The widespread use of high-speed cameras in examining fast-changing processes within the thematic scope of this work can be found in numerous scientific publications [14,15].

One of the main results of this work is the simulation model developed in the MSC ADAMS software, which was successfully verified based on the experiments conducted on the actual object [16,17]. The MSC ADAMS software used in this study is widely favored by researchers for modeling multi-body dynamic systems [18,19]. The results of this research illustrate the usefulness of the developed simulation model and provide opportunities for its use in further analyses of the impact of destructive (wear) processes on selected kinematic and dynamic parameters of the investigated mechanisms.

The literature also provides the possibility of validating mechanical properties using numerical models to confirm the acquired measurements [20] as well as examples of incorporating dynamic finite element methods to improve the simulation process [21]. Numerous investigations on internal ballistics are also available [22], but they are not within the intended scope of this work.

A further principal result of this work is the creation of a fuzzy-logic expert system in MATLAB leveraging the Fuzzy Logic Designer. The framework of fuzzy logic proposed by Zadeh [23] enables the modeling of uncertainty and imprecision in complex engineering systems. It has found applications in mechatronics [24]. It has likewise been employed in aviation [25,26]. Moreover, it has been utilized in medicine [27]. In the work, the controller was designed based on input signals representing variations cylinder gas pressure (pressure), the lubrication condition of the mechanism (friction) and changes in clearances within the kinematic chain of the device (clearance). The final stage of the work involved developing an application that, based on the input data, provided information about the condition of the device. The implemented code allowed the technician to determine whether the device was operational or non-operational and required maintenance actions.

The results of these studies will provide significant support in the operation process of specific types of objects under investigation. Despite the publication of many examples of the application of the software and research devices used in this work, the authors did not find any research results on the analyzed type of mechanism, which is distinguished by the specificity of its construction and operation, in the available literature.

MATERIALS AND METHODS

Research object

The researched mechanism utilizes the energy generated by propellant gases from a fired pyrotechnic charge, which are directed from the two conduits of the barrels to a gas distributor. The preparation for launching the pyrotechnic charge from the second barrel occurs by harnessing the energy of gases after the charge in the

first barrel is discharged. The driving elements of the mechanism are the sliders with gas stems. In Figure 1, the CAD assembly model of the analyzed system and its individual components are illustrated. The mechanism features two sliders (8) connected kinematically by connectors (10) and a connecting lever (3). During the operation cycle of the mechanism, each slider moves only in one direction (either backward or forward). The propellant gases are simultaneously delivered through openings in the barrel conduit to the space in front of the gas stem (15) retracting with the slider, as well as to the space behind the returning stem and slider. As a result of the propellant gases, the gas stems begin to move - one backward and the other forward. During the movement of the gas stems with the sliders, cam acceleration mechanisms are activated, comprising the slider, accelerator (12), connecting rod and bolt (13). One of these mechanisms uses the bolt to deliver a pyrotechnic round to the chamber, while the adjacent mechanism ejects the casing of the previously launched pyrotechnic round. The pyrotechnic round is locked in the chamber by the transverse movement of the bolt, which also functions as the element that feeds the pyrotechnic round. The cam mechanism is responsible for the smooth acceleration and deceleration of the bolt. To supply the mechanism with pyrotechnic rounds, a single belt is used, which is moved by the feeder star (19), kinematically connected by the connecting lever to the driving element of the mechanism. During one cycle of operation, the feeding assembly moves the belt with pyrotechnic rounds by one increment. Each pyrotechnic round is lowered by front and rear feeders (9 and 14) to the feeding line (i.e. to the bolt lugs). The feeders are kinematically connected to the sliders. The pyrotechnic rounds are sequentially fed by the bolts into each of the barrels [28]. The mechanisms described above, namely the accelerating and feeding mechanisms, are fundamental elements of the system and the focus of investigation in this work.

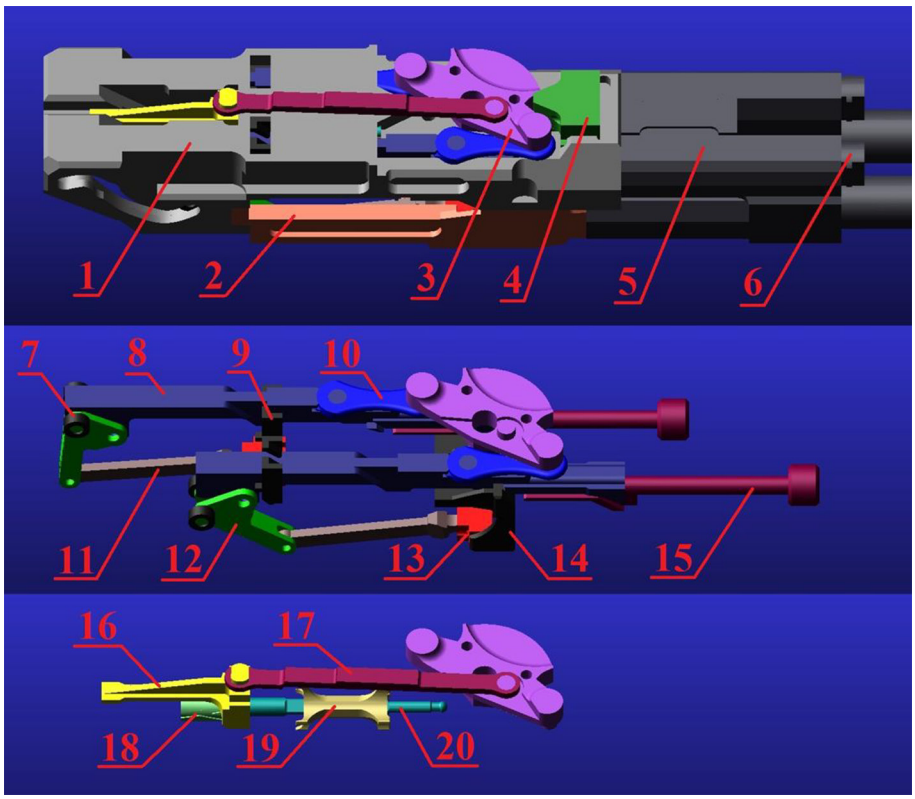

Figure 1. CAD assembly model of the analyzed mechanism and its individual components (own elaboration): (1) – Base of the lift, (2) – Lock chamber, (3) – Connecting lever, (4) – Anti–rebound, (5) – Gas distributor, (6) – Front plug, (7) – Accelerator roller, (8) – Slider, (9) – Rear feeder, (10) – Connector, (11) – Connecting rod, (12) – Accelerator, (13) – Bolt, (14) – Front feeder, (15) – Gas stem, (16) – Feeder collector, (17) – Feeder connecting rod, (18) – Feeder drum, (19) – Feeder star, (20) – Multi–Spline shaft

Field testing station

Experimental tests were conducted at the firing range. The research was conducted using a specially prepared apparatus (Figure 2), which included: the researched mechanism, its mounting elements with a transport platform, and equipment for measuring gas pressure in the gas cylinders.

As part of the preparations for pressure measurements [29], the original gas plugs (Figure 3a), which seal the gas cylinders at the barrel outlet, were removed from the tested mechanism. On the basis of their geometry, new components equipped with ports for pressure sensors were manufactured (Figure 3b). To track the gas pressure in the gas cylinders at the research platform, Kistler piezoelectric sensors (model no. 6215) were used, along with a signal converter, computer, and signal cables.

The prepared measurement system with installed and calibrated piezoelectric sensors [30] is shown in Figure 4.

RESULTS AND DISCUSSION

Measurement of powder gas pressure in gas cylinders

Measurement of powder gas pressure in gas cylinders using piezoelectric sensors enabled obtaining pressure-time profiles during shooting conducted in series of 2, 4, and 6 shots. During the experiments, measurements of gunpowder gas pressure in the gas cylinders were obtained (Figure 5). The chart illustrates the pressure values monitored by sensor No. 1 (located in the left gas cylinder) and sensor No. 2 (mounted in the right gas cylinder). The chart displays the pressure profiles within the gas cylinders, along with the duration of the pressure pulse that powers the mechanism, and the time gap between launching successive rounds (alternating between the left and right barrels), arising from the operational cycle of the mechanism. The chart also shows the maximum pressure values in the gas cylinders after launching rounds from the left and

Figure 2. Research platform at the experimental test range

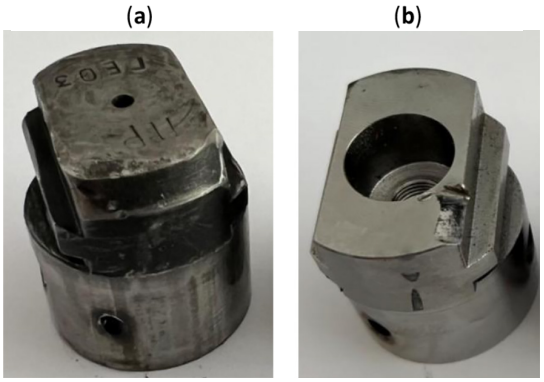

Figure 3. Photos of gas cylinder plugs: (a) original, (b) manufactured for research purposes

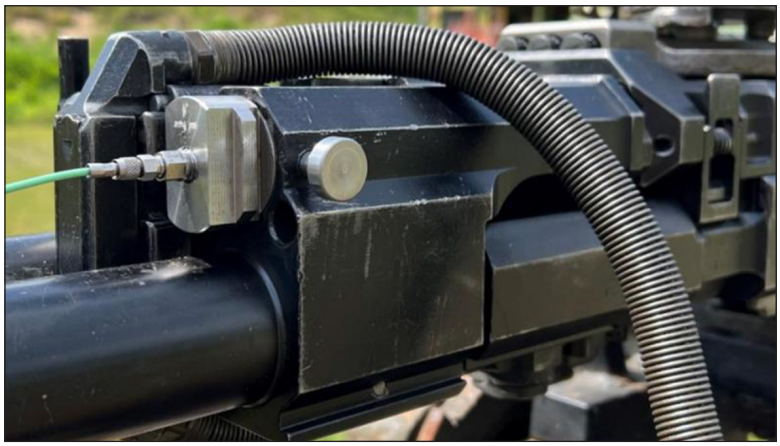

Figure 4. View of the gas cylinder plug manufactured for research purposes with the installed sensor and locking pin in the gas cylinder

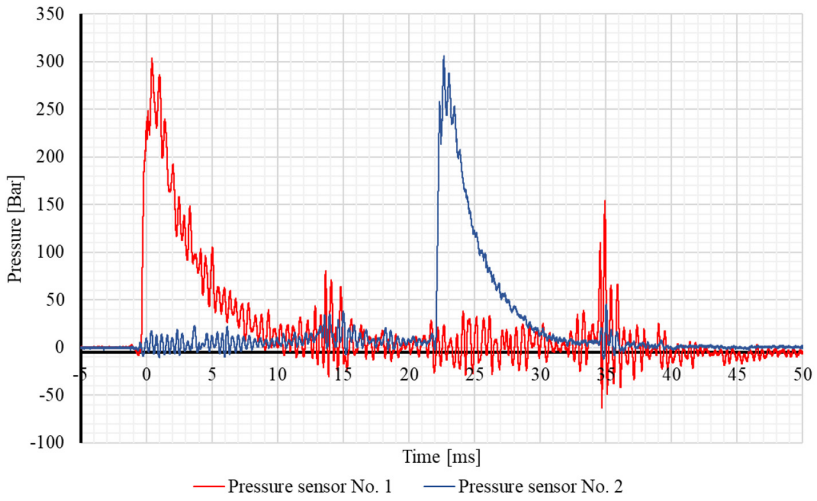

Figure 5. Gas pressure variation over time in the left and right gas cylinders (own elaboration)

right barrels [31]. The measurement results were compiled in Table 1.

Experimental research on the mechanism using a high-speed camera and TEMA CLASSIC software

During the experimental field tests, a FASTCAM SA-Z high-speed camera was used [32], along with a computer equipped with dedicated image acquisition software and TEMA CLASSIC software for motion analysis based on the recorded video sequences.

Before starting the measurements, the parts and mechanisms of the device the movement of which was visible from the outside and could be recorded with the high-speed camera, while maintaining a safe distance during the tests, were selected. The recordings were made with the optical axis of the camera lens positioned perpendicular to the longitudinal axis of the mechanism housing. The elements the movement of which was recorded included the feeder connecting rod (Figures 1–13) and the accelerator roller (Figures 1–6). The configuration for recording the displacements of selected elements of the cannon mechanisms is depicted in Figure 6.

In Figure 7, the initial position of the mechanism elements before starting its operation is depicted. After its pyro-technic initiation, the feeder connecting rod (Figure 7 – Point #1) moved along the longitudinal axis of the mechanism housing. The accelerator roller (Figure 7 – Point #2) moved according to the geometry of the

Table 1. Measurement results of gas pressure in the gas cylinders

Duration of the pulse [ms]	Time gap [ms]	Maximum pressure [Bar]	Measurement uncertainty [%]
16	21.7	307	± 0.5

Figure 6. The arrangement for recording the movement of mechanism elements during the tests

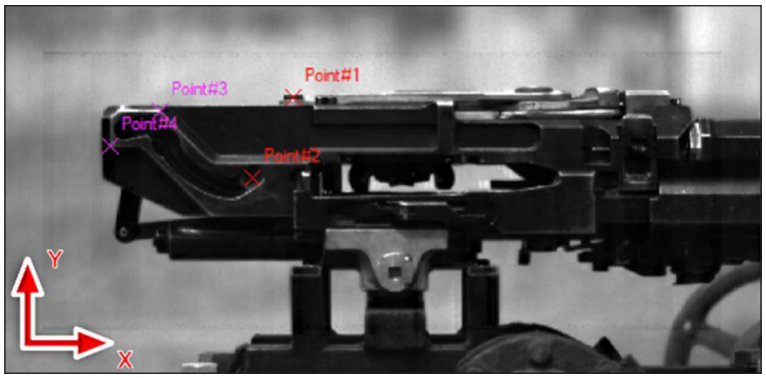

Figure 7. Visualization of the feeder connecting rod and accelerator roller in the initial position, i.e. at the foremost extreme position, along with the software-marked points the movement of which was recorded

accelerator cam (curvilinear slot serving as the roller guide). Throughout one operational cycle, the examined elements shifted from the foremost extreme position to the rearmost extreme position.

Additionally, points were marked in the software (Figure 7 – Point #3 and Point #4), which were used to convert the linear dimension measured during testing into a pixel-based dimension.

In Figure 8, the positions of the characteristic points (Figure 8 – Point #1 and Point #2) on the feeder connecting rod and accelerator roller are illustrated in the rearmost extreme position, at the end of the operational cycle.

The analysis of the displacement of points (Figure 7 and 8 – Point #1 and Point #2) conducted using TEMA CLASSIC software enabled visualization of the displacement changes of the feeder connecting rod and accelerator roller during a single operational cycle of the mechanism. Additionally, changes in the velocity of the tested elements during the operation of the system were determined.

Recording the displacement of cannon mechanism elements faced difficulties because of significant recoil of the mechanism body following the ignition of the pyrotechnic charge. To determine the displacement of the mechanism elements resulting from its operation, displacements caused by the recoil of the mechanism housing were subtracted from the displacement values of the mechanism elements. For this purpose, one of the points designated for converting linear dimensions (Figure 7 – Point #3) was utilized, leveraging its movement caused by recoil to correct the displacement of the tested components. To analyze and visualize the results on graphs, it was assumed that the horizontal axis aligns with the longitudinal axis of the housing, while the vertical axis is perpendicular to it.

Changes in displacement along the horizontal and vertical axis for the accelerator roller were illustrated in Figure 10. The analysis of the graph shows that the displacement of the accelerator roller from the foremost to the rearmost position is 104.5 mm, along the horizontal axis and 52.7 mm along the vertical axis. The displacement along the horizontal axis of the feeder collector displacement changes was illustrated in Figure 11.

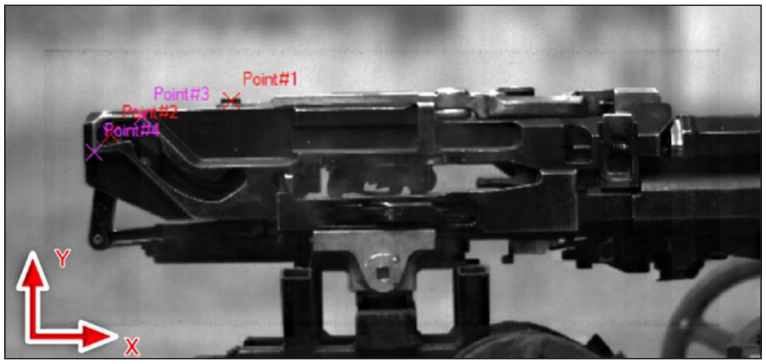

Figure 8. Visualization of the feeder connecting rod and accelerator roller in the rearmost extreme positions along with the new positions of the characteristic points located on the tested elements

Upon analyzing the depicted graph, it was found that the feeder collector moved 37.6 mm from its foremost to its rearmost extreme position.

Simulation of the mechanism operation using the MSC ADAMS software

As part of the research, computer simulations were conducted to analyze the operation of the mechanism using the MSC ADAMS software. 3D virtual models of individual mechanism components were created using Solid Edge based on geometric dimensions obtained by the authors through measurements of the components in the investigated configuration. The designed CAD model was subsequently implemented in the MSC ADAMS software. To account for the mass of individual mechanism components, the material density equivalent to that of steel, 7801 kg/m3, was adopted [33]. Next, the mutual relationships between interacting elements in each kinematic pair of the mechanism were defined to enable its operation in accordance with the functioning of an actual device. Additionally, for the cam mechanism, the interaction between the accelerator rollers and the base of the lift was defined using the contact function, enabling the simulation of the accelerator mechanism operation, ensuring smooth acceleration and deceleration of the bolt [34,35]. The adopted parameter values for the contact function are as follows: stiffness 1.0E+05 [N/m], force exponent 2.2 [N], damping 1.0E+04, penetration depth 1.0E-05 [m]. Additionally, a static friction coefficient of 0.1 and dynamic friction coefficient of 0.05 were applied to individual kinematic pairs. A crucial aspect of constructing the model was defining the driving force of the analyzed mechanism based on the results of field tests, which captured the variation in pressure values of propellant gases in the gas cylinders (Figure 5) during the operation of the actual device. With knowledge of the pressure variation and the diameter of the gas stem (f36 mm), it was possible to determine the profile of the driving force acting on the gas stem, which in turn moves the subsequent components of the mechanism. To define the driving component in the simulation model, a polynomial approximation of the driving force variation over time during the mechanism operation was performed. The approximation was performed using a third-degree spline function:

$$a + b \cdot t + c \cdot t2 + d \cdot t3 = 0 \qquad (1)$$

where: a, b, c, d – the coefficients of the polynomial, t – time.

Table 2 lists the coefficients of the polynomial approximating the force values expressed in Newtons, which vary over time expressed in milliseconds. The final approximating function consists of three spline curves with the polynomial coefficients specified in Table 2 for three intervals of time. The results of the approximation are presented in Figure 9, showing the variation in force derived from the measured pressure values and the graph of the force function resulting from the approximation.

The driving force defined by the polynomial for the analyzed mechanism was then

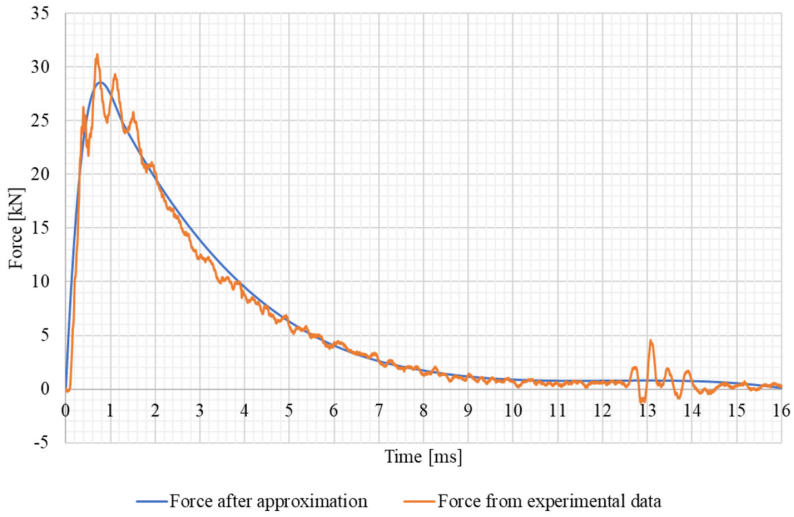

Figure 9. Graph of the force acting on the gas stem derived from experimental data and after polynomial approximation (own elaboration)

Table 2. Values of polynomial coefficients describing the profile of driving force over time

Polynomial coefficients	Time interval Δt 0–1.251 [ms]	Time interval Δt 1.252–7.931 [ms]	Time interval Δt 7.932–16 [ms]
a	-5452.591	34784.841	26237.951
b	99486.303	-9799.527	-6352.004
c	-91663.783	971.044	523.021
d	25545.189	-32.971	-14.296
Standard deviation	2074.929	427.390	621.931
Correlation coefficient	0.968	0.997	0.432

implemented in the MSC ADAMS software. The total duration of the motion input is 16 ms, corresponding to the duration of a single cycle of the mechanism operation. The method of modeling kinematics and dynamics of multibody systems used in the MSC ADAMS software enabled the simulation of the mechanism operation and the determination of displacements and velocities of selected model elements. The changes over time of the determined quantities were presented in Figures 10–11, allowing for their comparison with the results of experimental field tests.

Comparative analysis of experimental and simulation research results and discussion of outcomes

Next, the authors verified the numerical model and the conducted simulation-based research. Comparison was made between the displacement values of two mechanism components: the accelerator roller moving along the cam in the housing of the mechanism, and the feeder collector (the motion parameters of these components were determined in experimental investigations). The comparison included results obtained from the simulation of the device mechanisms in the MSC ADAMS software and results recorded during the experiment conducted using high-speed camera and the TEMA CLASSIC software.

The displacement results of the accelerator roller obtained through numerical simulation using the MSC ADAMS software are shown in Figure 10 (the accelerator roller moved 107.5 mm horizontally and 50.1 mm vertically). Meanwhile, the results obtained from numerical calculations of the feeder collector's motion parameters were presented in Figure 11 (it moved along the X-axis by 36.9 mm).

General agreement can be observed between the results obtained from high-speed camera measurements (TEMA) and numerical simulations (ADAMS). However, minor differences are present in certain areas. The agreement between the two characteristics of feeder collector is the best among the analyzed cases. The differences are minimal. The curves almost completely overlap throughout the time range. The difference in maximum displacement is less than 1 mm, which corresponds to a very small relative error.

Comparing all the characteristics, it can be concluded that the ADAMS model accurately reflects the real behavior of the system. The greatest agreement is observed for the feeder collector, while the largest discrepancies occur in the

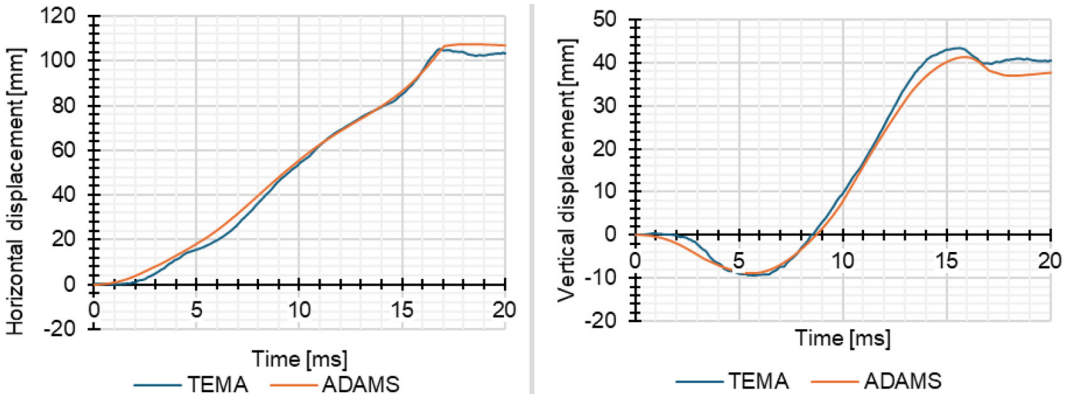

Figure 10. Displacement changes of the accelerator roller relative to the horizontal axis X and vertical axis Y

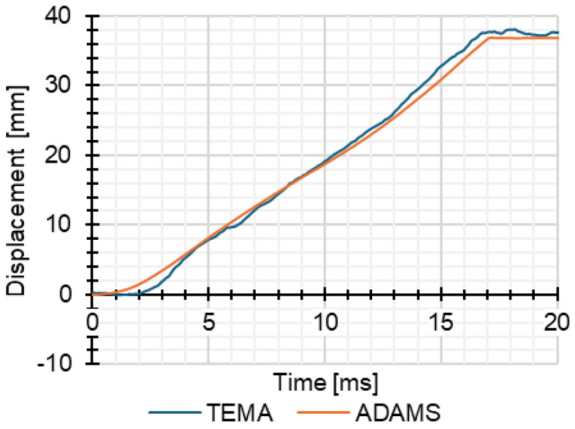

Figure 11. Change in displacement of the feeder collector over time

middle phase of displacement for the accelerator roller in the Y-axis.

It can be concluded that the kinematic characteristics of the accelerator roller and the feeder collector obtained experimentally and numerically are reasonably consistent. Therefore, the verified simulation model will be used in subsequent studies.

Investigations of the modeled mechanism

In subsequent research, the effects of selected design and operational parameters on the kinematic characteristics of the mechanism were analyzed. The initial phase of the research focused on investigating how variations in the force acting on the gas piston affected the device kinematics. Simulations were performed for scenarios with the driving force reduced by 10%, 20%, and 30%, as well as increased by the same percentages (Figure 12).

Changes in the driving force of mechanisms have a significant impact on the dynamics of all examined components. These changes affect both the time required to reach the maximum displacement and the shape of the curves describing the motion of individual elements. A logical pattern can be observed in the analyzed characteristics (Figure 13–14). An increase in the driving force (+10%, +20%, +30%) results in shorter operation times for the mechanisms and a more dynamic displacement profile. The mechanisms achieve their maximum displacements at a faster rate, which is reflected in the steeper slope of the curves during the initial time interval. Conversely, a decrease in driving force (-10%, -20%, -30%) results in longer operation times and a more gradual increase in displacement. However, the nature of these changes is not linear. A reduction in force by a certain percentage has a more noticeable effect on the motion time compared to a corresponding increase in force.

In the case of the accelerator roller, displacement changes are more pronounced. In the vertical axis, an oscillation effect is visible in the final phase of motion for lower force values. This may indicate reduced stability of component for lower force value. The characteristics suggest that accelerator roller is particularly sensitive to changes in driving force. This sensitivity is potentially due to its critical role in transmitting energy within the mechanism. The changes in motion dynamics for feeder collector are more subdued. The displacement characteristics are more consistent with each other. Higher force values result in faster achievement of maximum displacement, but the impact of force reduction is less drastic. This may suggest that the feeder collector is less sensitive to variations in driving force.

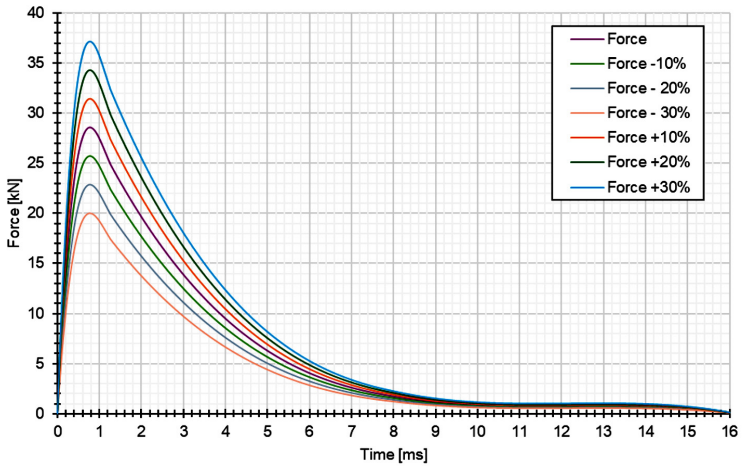

Figure 12. Change of the force acting on the gas stem over time (own elaboration)

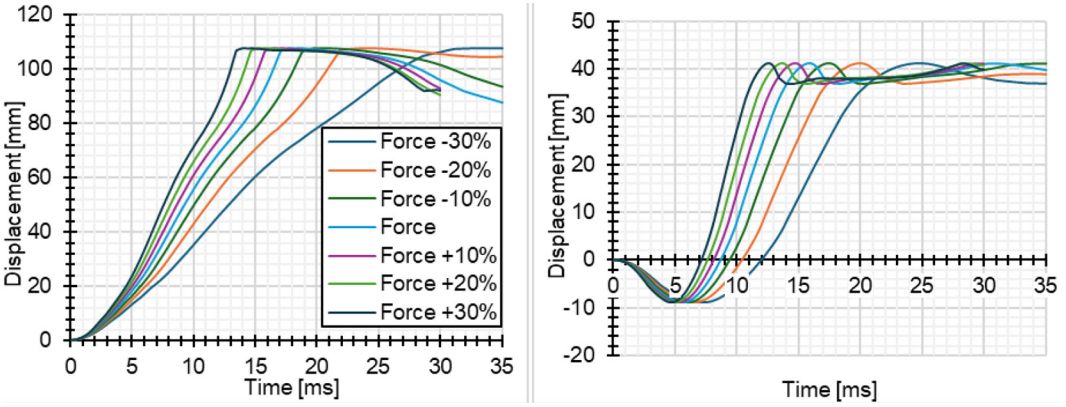

Figure 13. Displacement changes of the accelerator roller relative to the horizontal axis X and vertical axis Y for different values of force

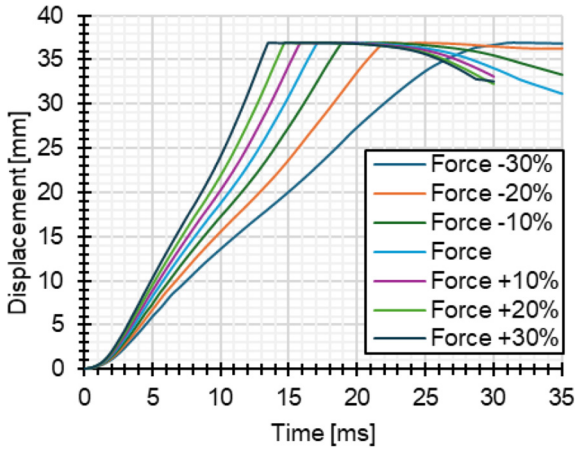

Figure 14. Change in displacement of the feeder collector over time for different values of force

In the next stage, the relationship between the mechanism kinematics and various friction coefficients in individual kinematic pairs was investigated [36]. Simulations were conducted under four scenarios depicted in Table 3. The first scenario assumed a dry mechanism. The second scenario involved a partially lubricated system. The third scenario considered a fully lubricated device. In the final scenario, simulations were performed without accounting for friction forces (Table 3).

The analysis of the following graphs (Figures 15–16) indicates a significant impact of friction on the dynamics of the mechanisms. In the non-lubricated condition (scenario 1), the mechanisms operate at the slowest pace. This results in an extended time to reach maximum displacement. Partial lubrication (scenario 2) improves the dynamics. It reduces the time required to reach maximum displacement. However, the differences between scenario 2 and scenario 1 remain moderate. For the fully lubricated device (scenario 3), the effects of friction are significantly reduced. This leads to a substantial decrease in the mechanism operating time. It also improves the dynamics. Maximum displacements are achieved much faster. The motion of the mechanisms becomes considerably more dynamic. The absence of friction (scenario 4) represents a theoretical scenario. In this case, the mechanisms achieve maximum displacements in the shortest possible time. The motion curves are the smoothest and most uniform.

Fuzzy logic reliability model

The proposed model is based on the Mamdani fuzzy controller in a MIMO configuration (Multiple Input, Multiple Output). Type-1 fuzzy logic was applied, where membership functions are precisely defined and take values in the range [0,1]. The simulation and experimental studies carried out as well as expert knowledge were used to determine both the number and the shape of the membership functions for input and output signals, as well as to design the rule base. With properly selected inference rules and an appropriate inference mechanism, the complete fuzzy modeling process can be carried out. Consequently, a fuzzy controller was developed.

In the designed model, the input signals represent the parameters that significantly affect the

Table 3. Friction coefficient values for four scenarios

Scenario number	Coefficient of static friction - μs	Coefficient of dynamic friction - μd
1	0.2	0.12
2	0.15	0.1
3	0.1	0.05
4	0	0

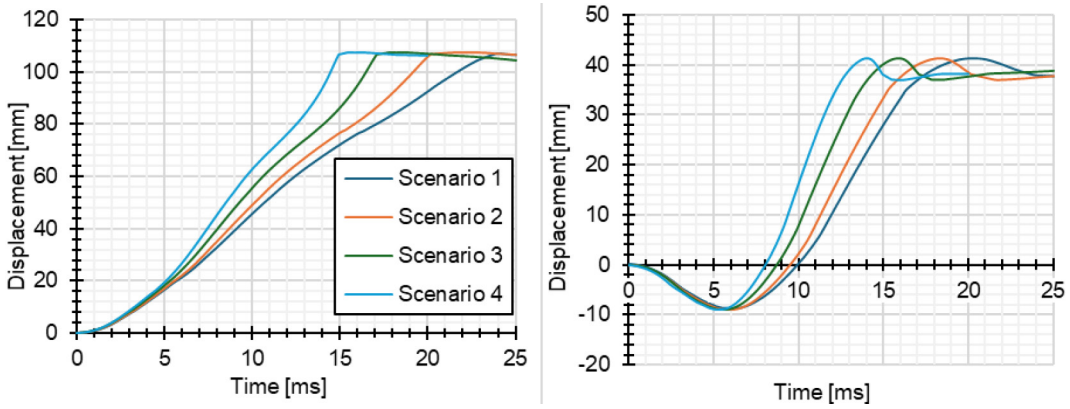

Figure 15. Displacement changes of the accelerator roller relative to the horizontal axis X and vertical axis Y for different values of friction

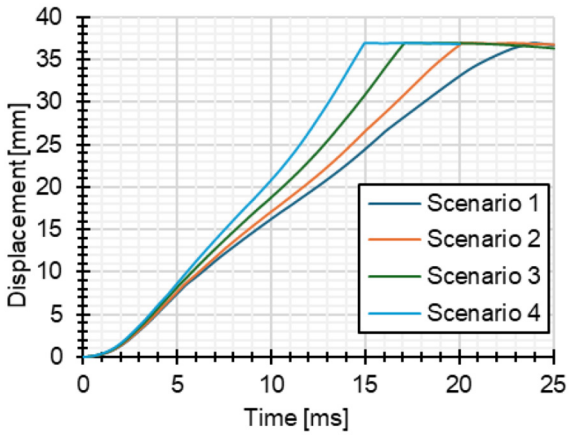

Figure 16. Change in displacement of the feeder collector over time for different value of friction

correct operation of the device: pressure (as the driving force source), friction (reflecting the level of lubrication in the mechanism), and clearance (increasing due to long-term operation). Seven membership functions were assigned to the first input parameter, while the second and third parameters were each described by four membership functions, defining the range and dynamics of their variations. The output signals include: time [ms] (converted into the operating speed of the device, represented by three membership functions) and the displacement [mm] of the slide and bolt (indicating either proper functioning of the mechanism or its jamming). All input and output membership functions were defined in a trapezoidal form. Their shapes and ranges are presented in Figures 17–22.

The next stage in designing the controller was the construction of the rule base. The total number of rules was determined by the number of possible variations of the input signals (Table 4). A change in pressure resulted in a simultaneous change of the driving force of the entire mechanism. The purpose of this modification was to observe how variations in the force acting on the gas piston influenced the kinematics of the device. The driving force was reduced by 10%, 20%, and 30%, and increased by the same percentages (7 membership functions). For friction, both static (μ s) and dynamic (μ d) friction coefficients in steel–steel contact were considered [36]. Four cases were defined to simulate the device under conditions of full lubrication, partial lubrication, no

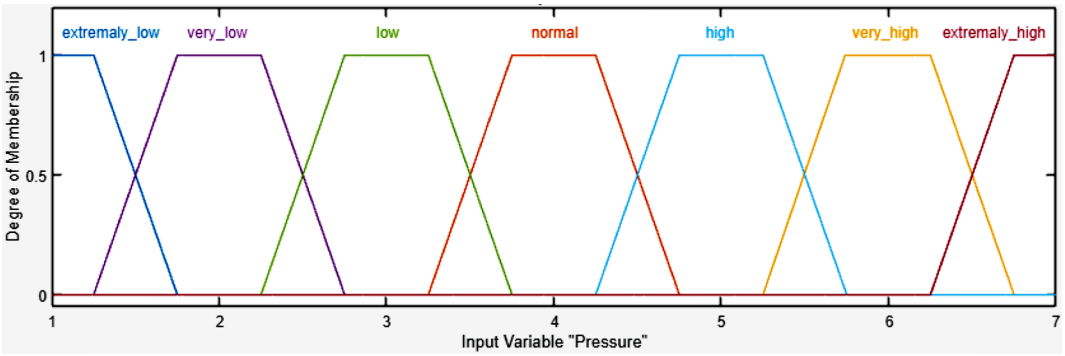

Figure 17. Membership functions and ranges of the input signal “Pressure”

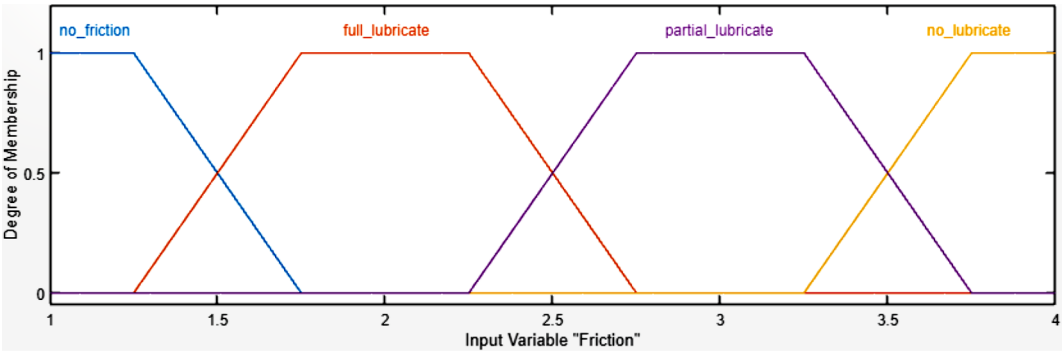

Figure 18. Membership functions and ranges of the input signal “Friction”

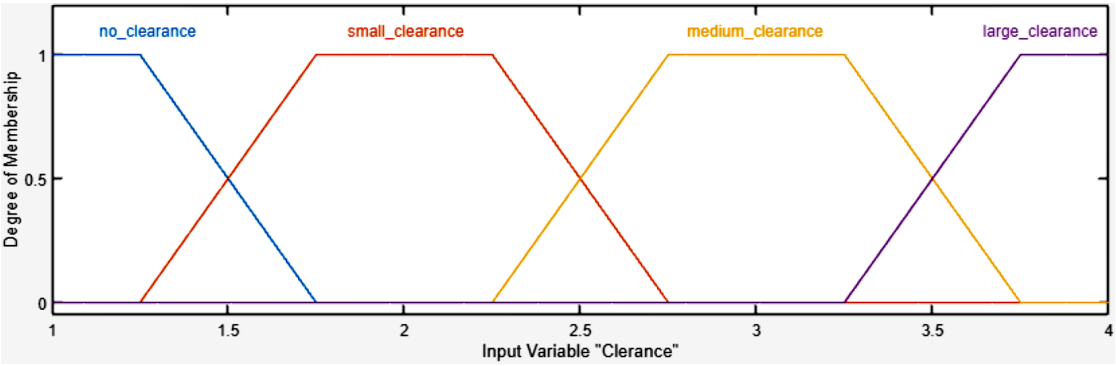

Figure 19. Membership functions and ranges of the input signal “Clearance”

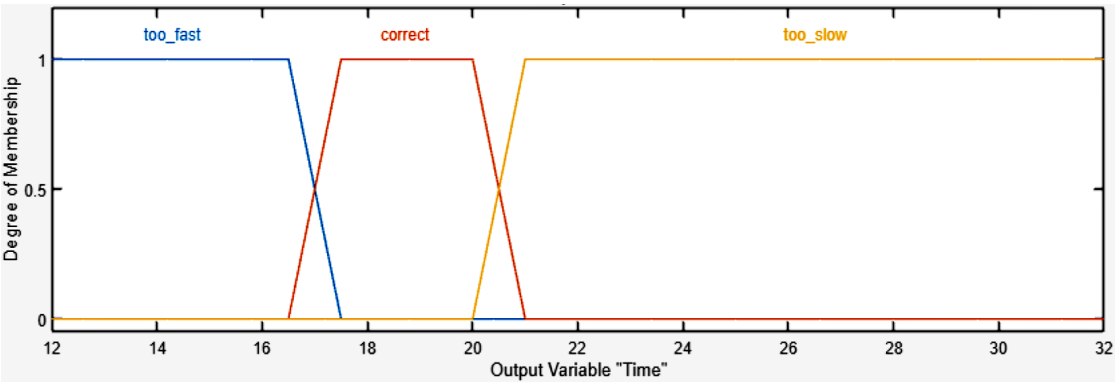

Figure 20. Membership functions and ranges of the output signal “Time”

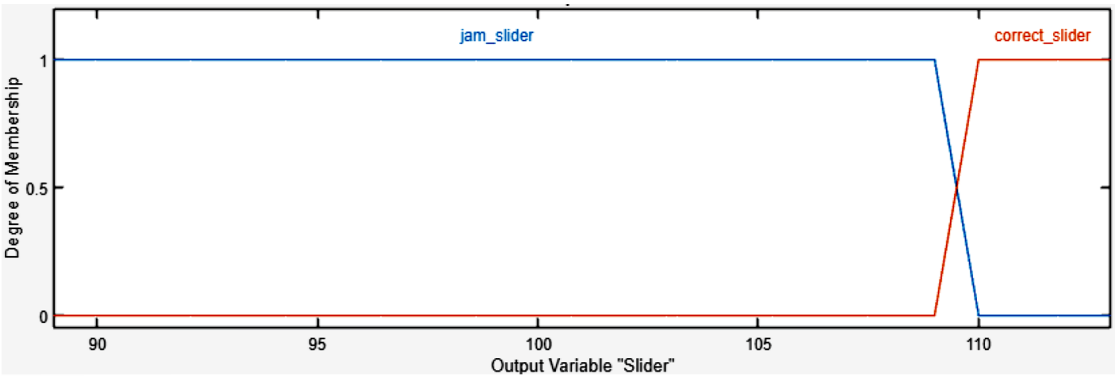

Figure 21. Membership functions and ranges of the output signal “Slider”

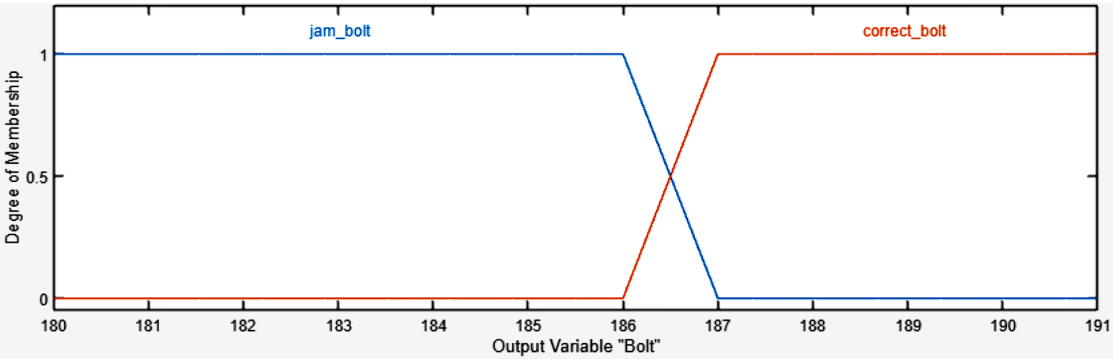

Figure 22. Membership functions and ranges of the output signal "Bolt"

Table 4. Membership function values of the input signals

Pressure		Friction	μ_s	μ_d	Clearance	
Extremely_low	-30%	No_friction	0.0	0.0	No_clearance	0
Very_low	-20%	Full_lubricate	0.1	0.05	Small_clearance	0.25
Low	-10%	Partial_lubricate	0.15	0.1	Medium_clearance	0.5
Normal	1	No_lubricate	0.2	0.15	Large_clearance	1
High	+10%					
Very_high	+20%					
Extremely_high	+30%					

lubrication and a state neglecting friction (4 membership functions). With respect to clearance, the kinematic chain responsible for delivering the power source to the chamber was analyzed. Particular attention was given to the kinematic pairs between the slide–accelerator, accelerator–connecting rod and connecting rod–bolt (Figure 1). Four variants were defined, representing clearances of 0.25 mm, 0.5 mm, 1 m and no clearance (4 membership functions). Importantly, the clearance values were intended to be measurable by the operator of the device. Subsequently, employing the validated simulation model of the mechanism in MSC Adams, a total of 112 simulations of the device operation were conducted.

From each conducted simulation, three critical parameters of the device were extracted. The first was the slider displacement [mm]. In accordance with the device operating guidelines [28], the instances at which the second derivative of the slider displacement reached zero were adopted as reference points defining either the completion of a full operating cycle or the occurrence of a malfunction. This criterion simultaneously provided an assessment of whether the slider had traversed the prescribed path. On the basis of the same reference instant, the second parameter was determined, namely the bolt position [mm]. Analogous to the slider, it was verified whether the bolt achieved the required travel distance or whether a jamming condition was encountered. The third parameter was the mechanism operating time [ms], which was analyzed to determine whether the mechanism performed its motion prematurely, within the admissible temporal range specified by the manufacturer, or excessively rapidly. On the basis of the simulations and the observed relationships between the input and output signals, 112 deduction rules were constructed. An example of such a rule is presented below: "If Pressure is EXTREMELY_LOW and Friction is NO_FRICTION and Clearance is NO_CLEARANCE then Time is TOO_SLOW, Slider is CORRECT_S, Bolt is CORRECT_B."

In the designed model, the basic methods of fuzzy inference were defined. The AND operator was implemented as the minimum function, so that a rule takes the value of the least satisfied condition. For the OR operator, the maximum method was applied, which selects the highest value among the alternative premises. In the implication part, the minimum method was used, whereas in the aggregation of results

from multiple rules the maximum method was adopted, corresponding to the logical summation of the effects of individual rules.

The system performance was analyzed using all available defuzzification methods: centroid, bisector, lom, mom, and som. Discrete values of pressure, friction, and clearance were introduced into the modeled system. The obtained results were then verified using fuzzy logic by comparing them with the outcomes of numerical simulations. The discrete values, after undergoing the inference and defuzzification process, were used to calculate the relative differences between the datasets. The comparison of results showed that the maximum-based methods (lom, mom, som) produced fewer stable outcomes, while the bisector method did not always reflect the actual behavior of the system. The best and most representative results were obtained with the centroid method; therefore, it was adopted as the primary defuzzification approach in the designed model.

To evaluate the performance of the designed fuzzy controller, so-called control planes were employed. This tool makes it possible to analyze how crisp input values are mapped onto the corresponding crisp output values across the entire range of parameters. The obtained control planes (illustrating the behavior of the model for operation time) are presented in Figures 23–25.

The analysis of the presented control planes confirms that the designed model accurately reflects the relationships between the input parameters and the operation time of the mechanism. The results are consistent with

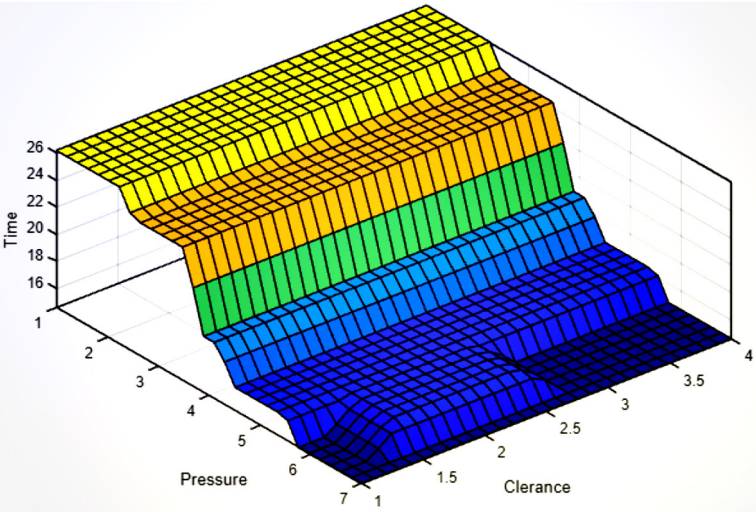

Figure 23. Influence of pressure and clearance on the operation time

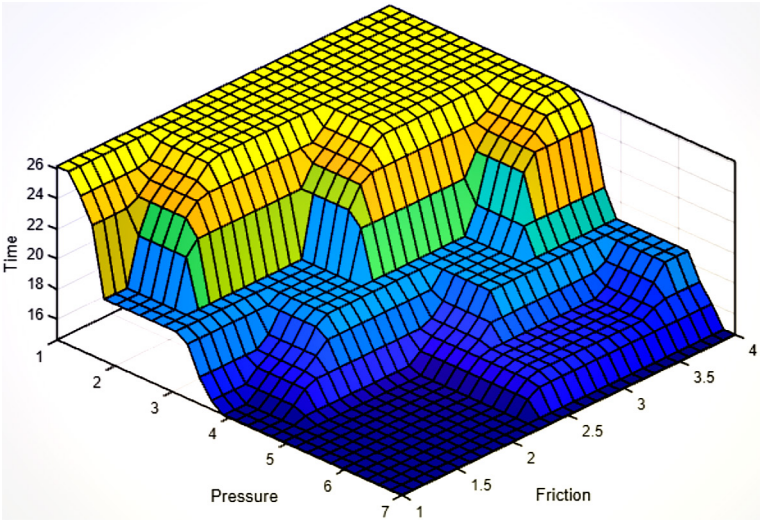

Figure 24. Influence of pressure and friction on the operation time

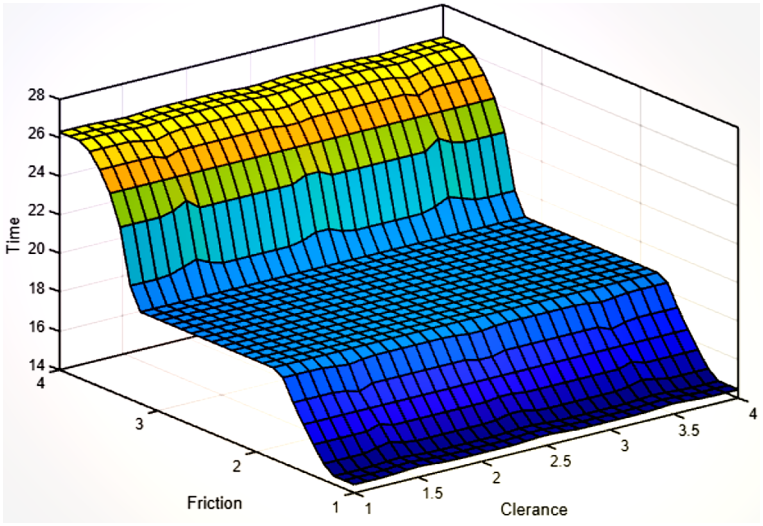

Figure 25. Influence of friction and clearance on the operation time

the manufacturer's data, which specify proper operation of the device within the range of time (17.6–20 ms) [28]. The most important conclusion is that the constructed controller enables the prediction of the mechanism behavior under non-nominal conditions.

Expert system model

The final stage of the work involved the development of an expert system designed to determine the technical condition of the mechanism – classified as either operational or non-operational. For this purpose, an application was implemented in the MATLAB environment, requiring the input of three parameters: pressure, friction and clearance, within a predefined range of values. The entered input data are processed within the fuzzy logic system. On the basis of the defined membership functions and inference rules, the output values are generated. The obtained results include the cycle time of the mechanism, the displacement of the slider and the bolt, as well as the admissible ranges of these quantities. Subsequently, the system automatically classifies the mechanism as either operational or non-operational. In the case of non-operational status, the user is additionally provided with information regarding the potential cause of the malfunction and the need for appropriate maintenance actions (Figure 26). If all parameters remain within acceptable ranges, the system – based on the outputs of the fuzzy logic module – confirms that the mechanism is operational (Figure 27).

Parameter	Measured value	Permissible range
Cycle time [ms]	26.30	17.6 - 20.0
Slider displacement [mm]	99.19	110 - 113
Bolt displacement [mm]	183.23	186 - 191

MECHANISM NON-OPERATIONAL

· *Cycle time is too long*
· *Slider displacement is out of range*
· *Bolt displacement is out of range*

Maintenance required

Figure 26. View of the application when the mechanism is assessed as non-operational

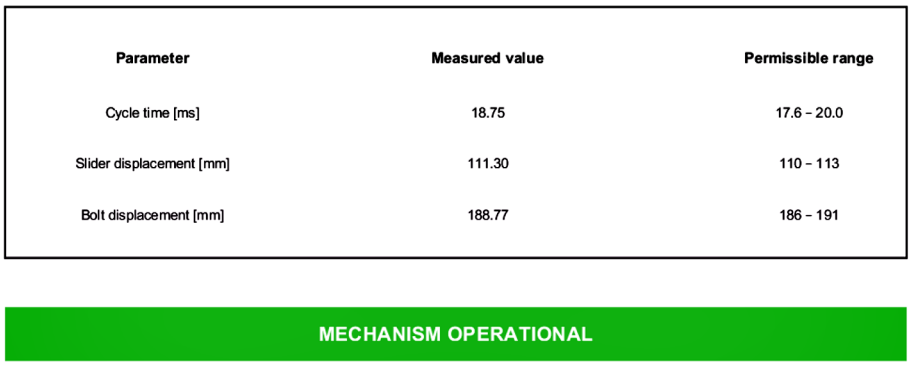

Figure 27. View of the application when the mechanism is assessed as operational

CONCLUSIONS

In this research project, experimental and numerical investigations were conducted to build a reliable simulation model of a pyrotechnically actuated automatic mechanism. This model will be used in further research to support the operational process. During the experimental research in the form of field tests measurements of propellant gas pressure in the gas cylinders of the mechanism were taken throughout its operational cycle. The obtained pressure values were used to determine the driving force for the successive kinematic components of the mechanism modeled in the MSC ADAMS simulation environment.

Simultaneously, during the experimental tests, displacements of the examined mechanism parts were recorded using a high-speed camera FASTCAM SA-Z. Motion analysis was conducted using dedicated TEMA software, which enabled the analysis of recorded images and precise tracking of the motion of selected kinematic components.

The kinematic characteristics obtained from numerical simulation investigations are reasonably consistent with the experimental results obtained from high-speed camera analysis processed with TEMA software. Therefore, the results of this research demonstrate the utility of the created simulation model and open possibilities for its application in further analyses of the impact of destructive (wear) processes on selected kinematic and dynamic parameters of the examined mechanisms.

The effect of selected design and operational parameters on the kinematic characteristics of mechanism was determined. The change in driving force significantly affects the dynamics of examined components. A reduction in force results in an extension of operation time and decrease in stability. The lubricated scenario (2) and (3) significantly improve the dynamics of the mechanisms, bringing their characteristics closer to the ideal scenario (scenario 4).

The last stage of the work involved the development of a fuzzy controller using Matlab software. On the basis of the simulation and experimental studies of the mechanism and expert knowledge, a controller utilizing fuzzy logic was designed. The practical applicability of the conducted research enabled the development of Matlab code that allows determining whether the device is operational or non-operational. The developed application assesses whether the output parameters of the device – such as the operation cycle and the displacements of selected components – remain within acceptable limits. If these values exceed the permissible thresholds, the technician is notified of the need to perform the required maintenance actions. The results of these efforts will serve as a foundation for further research and provide significant support in the operational process of a specific class objects that are the focus of the authors' work.

Acknowledgements

This research was funded by Military University of Technology (Warsaw, Poland) under research project UGB 531-000036-W200-22/2025.

REFERENCES

1. Damaziak K, Płatek P, Małachowski J, Woźniak R. Analysis of the potential use of various numerical methods in the design process of a 5.56 mm caliber firearm automation system. Mechanik. 2011; 84(2), 120–123.
2. Jasztal M. The method of modeling and examining mechanical assemblies of selected aircraft armament

devices. Mechanical Review no. 4/06, 15–20.

3. Jasztal M. The use of CAD/CAE systems in the research of aircraft armament components. In: Wetoszka A, Truskowski A, eds. Selected Aspects of Combat Aviation Application. The Publishing House of the Air Force Academy: 2017.
4. Damaziak K, Małachowski J, Płatek P, Woźniak R. Numerical studies of the dynamic response of a standard rifle auto-mation system. Bulletin MUT. 2012; LXI, No 3: 181–194.
5. Yang H, Xu J, Wang G, Yang Z, Li Q. Prestress modal analysis and optimization of cantilever supported rotor under the unbalanced axis force and moving mass. Applied Sciences. 2022; 12(10): 4940.
6. Jasztal M, Kunikowski M. Modelling and simulation of functioning of the GSh-23 aviation autocannon mechanisms. Technical Sciences. 2021: 24(1).
7. Rośkowicz M, Jasztal M, Kunikowski M. The experimental-numerical study of aviation autocannon mechanisms. Problems of Mechatronics. Armament, Aviation, Safety Engineering 2024; 15(2): 101–118.
8. Krause T, Kanbur H, Springer N, Brunzendorf J, Markus D, Walch O, Heer C. Acceleration sensitivity of piezoelectric pressure sensors and the influence on the measurement of explosion pressures. Journal of Loss Prevention in the Process Industries: 2023.
9. Bieniek P, Weiss J. Methods of measuring maximum propellant gas pressure used during firing from a position equipped with a 120 mm cannon of the Leopard 2A4 tank. Problems of Armament Technology: 2019.
10. Hu J, Chen H, Yu Y, Xue X, Feng Z, Chen X. Experimental study on motion law of the fragment at hypersonic speed. Processes. 2023; 11(4): 1078.
11. Su B, Yao X, Wang P, Bian X, Cui X. Experimental research on impact effect of high-speed water jet acting on a rigid target with attached water layer. Ocean Engineering: 2023.
12. Xu L, Cheng C, Du C, Jiang Z, Du Z, Gao G. Semicrystalline polymers applied to taylor impact test: Constitutive, experimental and FEM analysis. Polymers. 2020; 12(7): 1615.
13. Si P, Liu Y, Yan J, Bai F, Huang F. Ballistic performance of polyurea-reinforced ceramic/metal armor subjected to projectile impact. Materials. 2022; 15(11): 3918.
14. Alagumalai V, Shanmugam V, Balasubramanian NK, Krishnamoorthy Y, Ganesan V, Försth M, Sas G, Berto F, Chanda A, Das O. Impact response and damage tolerance of hybrid glass/kevlar-fibre epoxy structural composites. Polymers. 2021; 13(16): 2591.
15. Ćwiklak J, Kobiałka E, Goś A. Experimental and numerical investigations of bird models for bird strike. Analysis. En-ergies. 2022; 15(10): 3699.
16. Guo D, Xie Z, Sun X, Zhang S. Dynamic modeling and model-based control with neural network-based compensation of a five degrees-of-freedom parallel mechanism. Machines. 2023; 11(2): 195.
17. Zhu X, Deng Y, Zheng X, Zheng Q, Liang B, Liu Y. Online reinforcement-learning-based adaptive terminal sliding mode control for disturbed bicycle robots on a curved pavement. Electronics. 2022; 11(21): 3495.
18. Tarnita D, Geonea ID, Pisla D, Carbone G, Gherman B, Tohanean N, Tucan P, Abrudan C, Tarnita DN. Analysis of dynamic behavior of ParReEx robot used in upper limb rehabilitation. Applied Sciences. 2022.
19. Cachumba-Suquillo S J, Alfaro-Ponce M, Torres-Cedillo S G, Cortés-Pérez J, Jimenez-Martinez M. Vehicle dynamics in electric cars development using MSC Adams and artificial neural network. World Electric Vehicle Journal. 2023; 14(10), 293.
20. Kosiuczenko, K., Simiński, P., Gmitrzuk, M., Nowakowski, M. Experimental and numerical validation of an armor plate test stand. Advances in Military Technology, 2024; 19(1): 55–69.
21. Wang, J., Xiong, S., Wen, Y., Wang, Y. Numerical simulation of actuation processes and decoupling pyroshock of a pressure cartridge-type pin puller. Journal of Low Frequency Noise, Vibration & Active Control. 2023; 42(3): 1363–1378.
22. Turkyilmazoglu, M. Cooling of particulate solids and fluid in a moving bed heat exchanger. Energy, 2020; 203: 117837.
23. Zadeh, L.A. Fuzzy Sets. Inf. Control 1965; 8: 338–353
24. Precup, R. E., Nguyen, A. T., Blažič, S. A survey on fuzzy control for mechatronics applications. International Journal of Systems Science, 2023; 55(4): 771–813.
25. Żyluk, A., Kuźma, K., Grzesik, N., Zieja, M., Tomaszewska, J. Fuzzy logic in aircraft onboard systems reliability evaluation—A new approach. Sensors, 2021; 21(23).
26. Dagal, I., Mbasso, W.F., Ambe, H. et al. Adaptive fuzzy logic control framework for aircraft landing gear automation: optimized design, real-time response, and enhanced safety. Int. J. Aeronaut. Space Sci. 2025.
27. Nambison NK, Singh DP, Mehar R, Nambison SN, Sharma H, Sharma D, Nambison E. Pathology report interpretation and disease diagnosis using fuzzy logic embedded in an artificial intelligence framework: A new paradigm for digital technologies. Cureus. 2024 Oct 9; 16(10): e71148.
28. Air Force Command. 23mm Aircraft Autocannon GSz-23Ł, Technical Specifications and Maintenance, no. 2750/88, Poznań: 1990.

29. Research procedure: LBUSO.PB.20. Measurement of propellant gas pressure using piezoelectric method: 3/6.03.2020.
30. Kistler Group. Instruction Manual: Charge Meter Type 5015A: 2010.
31. Research report 1/2023-200/2000/WAT/2023
32. https://www.brj.pl/wp-content/uploads/2018/06/photron-fastcam-sa-z-2017.pdf
33. Bankowski Z. I in. A small guide for mechanics, Scientific and Technical Publishing 1985; 224(24).
34. Giesbers J. Contact mechanics in MSC Adams – A technical evaluation of the contact models in multibody dynamics software MSC Adams. University of Twente: 2012.
35. Sapietová A, Gajdoš L, Dekýš V, Sapieta M. Analysis of the influence of input function contact parameters of the impact force process in the MSC. ADAMS. In: Advanced Mechatronics Solutions (pp. 243–253). Springer International Publishing: 2016.
36. Fischer, U., Heinzler, M., Näher, F., Paetzold, H., Gomeringer, R., Kilgus, R.,..., Stephan, A. Mechanic's Handbook. REA Publishing. 2009.